

Fractional Stokes–Einstein Relationship in Biological Colloids: Role of Mixed Stick–Slip Boundary Conditions

G. Chirico,[†] M. Placidi,[‡] and S. Cannistraro^{*,‡}

Instituto Nazionale Fisica della Materia and Dipartimento di Fisica dell'Università, I-20133 Milano, Italy, Dipartimento di Fisica dell'Università, I-06100 Perugia, Italy, and Dipartimento di Scienze Ambientali, Università della Tuscia, I-01100 Viterbo, Italy

Received: June 25, 1998

The bovine serum albumin mutual diffusion coefficient D has been measured by photon correlation spectroscopy as a function of protein concentration. The solution viscosity η_{sol} has been obtained by following the diffusion of spherical probes added, at a small volume fraction, to the protein solution. It is found that D follows a fractional Stokes–Einstein relation $D \sim 1/\eta_{\text{sol}}^\alpha$ with $\alpha \approx 0.5$ up to a protein concentration $C \approx 15$ g/dL. The observed behavior has been traced back to interparticle interactions taking into account the possibility of mixed stick–slip boundary condition at the protein–water interface.

I. Introduction

The Stokes–Einstein (SE) relation connects, in a highly diluted solution, the mutual diffusion coefficient D of colloidal particles of radius R to the solvent viscosity η_0

$$D = \frac{k_B T}{6\pi\eta_0 R} \quad (1)$$

This applies also to proteins, and indeed the SE relation has been the basis for many important studies of their size and shape in solution.¹

One of the most powerful techniques to measure the protein diffusional properties is photon correlation spectroscopy (PCS). From the relaxation time of the autocorrelation function of the scattered light one measures the mutual diffusion coefficient of the colloidal particle D and relates this to the solvent viscosity η_0 . Deviations from eq 1 have been reported in glass forming liquids^{2,3} and in semidilute or concentrated protein solutions.⁴ As a matter of fact, colloidal and polymer systems when studied as a function of solute concentration^{5–7} at isothermal conditions, show some analogies with glass forming liquids. The physical properties of concentrated biopolymer solutions play a major role in the understanding of several physiologically relevant phenomena, such as diffusion controlled macromolecular reactions⁸ or protein concentrated solutions that can even show phase transitions.⁹ In some cases a fractional relation between the diffusion coefficient and the solution viscosity has been reported:^{8,10,11}

$$D = \frac{k_B T}{6\pi\eta_{\text{sol}}^\alpha R} \quad (2)$$

with $\alpha < 1$, where the solution viscosity, which is significantly dependent on the protein concentration, must be measured at a low shear rate due to the non-Newtonian character of polymer solutions. A suitable approach is to measure the solution

viscosity by inverting the SE relation for a large colloidal particle (e.g., latex sphere) dispersed at very low volume fraction in the biopolymer solution.^{12,13} Then, by means of PCS measurements alone it is possible to relate the protein mutual diffusion coefficient D and the solution viscosity η_{sol} .

In the present work we measure the extent of the deviation from the classical SE relation for a protein solution and give an interpretation of this behavior based on the study of the perturbations of the solvent velocity field induced by the fluctuations in the protein number density. The perturbations of the solvent velocity field are involved in the complex solvent–colloid interaction and, though dependent also on the particular “corrugated” protein surface,^{3,4} are mainly due to the displacement of solvent volume induced by the protein diffusive motion.

Since these protein–solvent interactions take place also in a perfectly homogeneous solvent, they can be regarded as an unspecific component which might contribute to the fractional behavior of the SE relation. The aim of the present work is to ascertain to what extent the observed behavior can be traced back to interparticle interactions taking into account the possibility of mixed stick–slip boundary condition at the protein–water interface.

The main result is to show that, at least up to $C \approx 15$ g/dL, the behavior of D versus η_{sol} follows a fractional Stokes–Einstein (SE) relation with $\alpha \approx 0.46$, and that this trend is compatible with an increasing slip-character of the water diffusion around the proteins at higher volume fractions.

II. Materials and Methods

The sample studied is bovine serum albumin (BSA) in acetate buffer at the isoelectric pH = 4.7 and at high ionic strength (0.1 M NaCl) in order to minimize electrostatic interactions. Gel-filtration chromatography was used to obtain monomeric BSA fraction, whose concentration was determined spectrophotometrically by using an absorptivity value of 6.67 dL/g cm at 280 nm. The mutual diffusion coefficient D of BSA (which has an almost spherical shape of radius ≈ 35 Å) has been obtained by photon correlation spectroscopy which measures the time autocorrelation function (ACF) of the photocounts due

* Author to whom correspondence should be addressed. E-mail: cannistraro@pg.infn.it.

[†] Dipartimento di Fisica dell'Università, Milan, Italy.

[‡] Dipartimento di Fisica dell'Università, Perugia, Italy.

to the light scattered by the sample:

$$\langle n(0)n(t) \rangle = \langle n \rangle^2 [1 + A |g^{(1)}(t)|^2] \quad (3)$$

where $n(t)$ is the number of photons counted, for a given scattering angle θ , at a time t for a sampling time Δt ; $\langle n \rangle^2$ is the value assumed from the time autocorrelation function for $t \rightarrow \infty$; A is a spatial coherence factor depending upon various experimental conditions, such as the coherence and receiver area, and $g^{(1)}(t)$ is the first-order normalized correlation function of the scattered electric field. In fairly monodisperse samples, the function $g^{(1)}(t)$ decays as a single exponential and eq 3 takes the form:

$$\langle n(0)n(t) \rangle = \langle n \rangle^2 [1 + Ae^{-2\Gamma t}] \quad (4)$$

the diffusion coefficient D is extracted from the decay constant Γ :

$$\Gamma = Dq^2 \quad (5)$$

where q is the amplitude of the exchanged wave vector given by $q = (4\pi n/\lambda) \sin(\theta/2)$; λ and n being the incident light wavelength and the solution refractive index, respectively. Γ has been obtained by fitting eq 4 with the method of the cumulants,¹⁴ by limiting the analysis to the second cumulant K_2 . A normalized second cumulant $K_2/\Gamma^2 < 0.06$, characteristic of a narrow distribution of decay times, has been obtained at all the concentrations investigated.

The low-shear viscosity of BSA solutions has been extracted from the translational diffusion coefficient D_p , of spherical probes (polystyrene spheres of radius $R_p = 57$ nm, Sigma Chemical) through the Stokes–Einstein relationship:

$$\eta_{\text{sol}} = \frac{k_B T}{6\pi R_p D_p} \quad (6)$$

which is known to be valid for large particles in the hydrodynamic limit such as dilute solution of polystyrene spheres.¹⁵ The spheres were diluted to a volume fraction $\phi_{\text{probe}} = 10^{-5}$ in the protein solution: this fraction represents the minimum for obtaining a good enough signal to noise ratio in the measured autocorrelation function without perturbing the system; in fact, it was much less than the minimum protein volume fraction $\phi \geq 0.02$. Under these conditions, due to the high scattering power of the latex particles, most of the scattered signal is due to the few suspended tracer particles. Actually, the intensity ratio I_{BSA}/I_p of the scattered light resulted to be about 3×10^{-2} . As a consequence, the contribution to the ACF from the BSA macromolecules comes out to be negligible and the ACF results to be very close to a single exponential. This is shown in the inset of Figure 1, where the ACF obtained under these experimental conditions is reported in a log scale. For sake of completeness, in the same figure, the ACFs obtained from a bare BSA solution (open circles) and from a binary mixture of BSA and Latex spheres (full circles) are reported after having been normalized. In both solutions the protein concentration was 10 g/dL. As it can be seen, the two ACF are located at significantly different time scale as due to the large difference in the diffusion coefficient of these two colloidal species; therefore, a tiny perturbation is expected in the ACF of the binary mixture. As a last remark, this method insures that viscosity measurements were carried out at low shear rate, which is an essential condition in non-Newtonian liquids such as protein solutions.

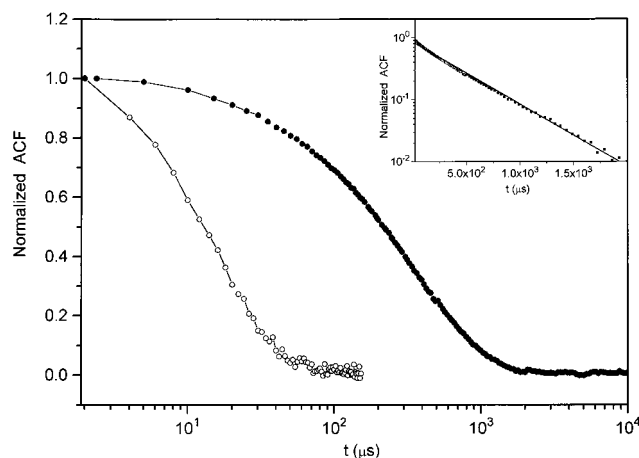


Figure 1. Normalized ACF of the scattered light intensity from a BSA solution (open circles) and from a binary mixture of BSA and Latex spheres (full circles). In both samples the protein concentration was 10 g/dL. The relative intensity $I_{\text{BSA}}/I_p \approx 3 \times 10^{-2}$. Inset: ACF measured in the binary mixture. The continuous line is a best fit to the experimental data with a single exponential function.

In all experiments, a $\theta = 90^\circ$ scattering geometry and a He–Ne laser light source running at 632.8 nm (35 mW optical power) have been used. The scattered light was detected by a photomultiplier and then passed to a BI-9000 (Brookhaven Instruments) digital correlator. All the measurements have been performed at 20.0 ± 0.1 °C on samples previously treated with $0.22 \mu\text{m}$ Millipore filter to avoid the presence of dust.

III. Theoretical Background

The general relation for the diffusion coefficient of a dilute solution of spheres of radius R in a solvent of viscosity η_0 under mixed stick–slip boundary conditions is¹⁶

$$D_0(\xi) = \frac{k_B T}{6\pi\eta_0 R(1 - \xi)} \quad (7)$$

where the parameter ξ characterizes the boundary condition and takes the values $0 \leq \xi \leq 1/3$. The two extremes $\xi = 0$ and $\xi = 1/3$ correspond to the complete stick and slip boundary conditions respectively. A simple generalization of the eq 7 to the mutual diffusion coefficient $D(C)$, i.e., to cases when the protein concentration C is not negligible, is a delicate matter as we will see in the following. In these cases, direct electrostatic or hydrodynamic interactions, the former dependent mainly on the solution pH and ionic strength I and the latter arising from the shear flow field by the Brownian particles, could play a role in determining the behavior of the mutual diffusion coefficient versus the protein concentration.

As a matter of fact, even if the proteins bore vanishing net charge, the excluded volume effects, coupled to the hydrodynamic interactions, are expected to give some contribution to the mutual diffusion coefficient at protein volume fractions as high as 10%. The effects of such interactions can lead to a power law relation between the solution viscosity η_{sol} and the diffusion coefficient D different from the simple SE relation.

The formal generalization of the eq 7 to finite protein concentration and to mixed boundary conditions can be obtained from the generalized SE equation

$$D(C, \xi) = \frac{M}{N_{\text{av}} f(C, \xi)} \left[\frac{\partial \Pi(C, \xi)}{\partial C} \right]_{p,T} \quad (8)$$

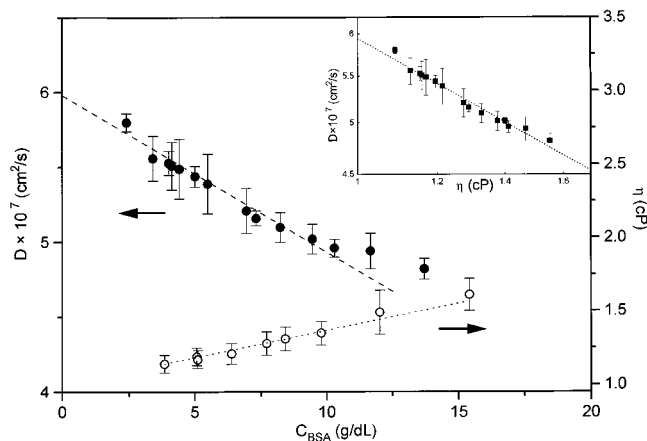


Figure 2. BSA mutual diffusion coefficient D (solid circles) and solution shear viscosity η (open circles) as a function of the protein concentration. The dashed and the dotted line are the best fit to the experimental data of D and η according to eqs 10 and 11, respectively. Inset: D vs η in a log–log scale. The continuous line is the best fit to the experimental data with a power law $D\eta^\alpha = \text{constant}$.

where $\Pi(C)$ is the osmotic pressure of the molecular solution, $f(C)$ is the effective friction coefficient which takes into account for the hydrodynamic interactions, M is the molecular weight, and N_{av} is the Avogadro number. Both $\Pi(C)$ and $f(C)$ can be expanded¹⁷ in series of C :

$$\left\{ \begin{array}{l} \Pi(C) = k_B T N_{\text{av}} M^{-1} [C + k_p C^2 + O(C^3)] \\ f(C) = f_0 [1 + k_f C + O(C^2)] \end{array} \right\} \quad (9)$$

where k_p is a purely thermodynamic term arising from the direct interactions and k_f describes the effects of hydrodynamic interactions between the particles. Then the mutual diffusion coefficient $D(C)$ may be written as

$$D(C, \xi) = D_0(\xi) (1 + k_D(\xi)C + O(C^2)) \quad (10)$$

where $D_0(\xi) = k_B T / (f_0(1 - \xi))$ and $k_D(\xi) = k_p - k_f$ is the diffusion interaction constant which may depend also on the type of boundary conditions.

The same type of expansion is possible for the viscosity of dilute and semidilute solutions of macromolecules¹⁸

$$\eta_{\text{sol}}(C) = \eta_0 (1 + [\eta]C + O(C^2)) \quad (11)$$

where $[\eta]$ is the intrinsic viscosity of the polymer, mainly dependent on the molecular hydrated mass (M_h) and volume (V_h). On the other hand, the parameter k_D does depend also on the interaction properties between proteins in solutions.¹⁶

IV. Results and Discussion

In Figure 2 the trend of the mutual diffusion coefficient D and the solution viscosity η_{sol} is shown versus C up to ≈ 15 g/dL. The dotted lines are the best fit to the data obtained using eqs 10 and 11 and give $k_D = -0.019 \pm 0.002$ dL/g, $D_0(\xi) = (5.97 \pm 0.02) \times 10^{-7}$ cm²/s, and $[\eta] = 0.040 \pm 0.003$ dL/g. The value $D_0(\xi)$ corresponds to the diffusion coefficient obtained under conditions of vanishing protein concentration and gives an hydrodynamic radius, $R_h = k_B T / 6\pi\eta_0 D_0 = 35.9 \pm 0.1$ Å.

For spherical shape, the radius of the molecule can also be calculated through

$$R_v = \left(\frac{3M\bar{v}}{4\pi N_{\text{av}}} \right)^{1/3} \quad (12)$$

By assuming an anhydrous protein mass $M = 69000$ daltons and $\bar{v} = 0.733$ cm³/g,¹ we find $R_v = 28$ Å which is consistently lower than R_h . The difference between the hydrated protein radius and R_v corresponds to approximately three water shells where the solvent molecules are influenced by the hydrodynamic shear motion of the protein. This simple consideration supports the assumption of stick boundary condition implicit in the derivation of R_h . However, the possibility of some degree of slipping of the water molecules in the vicinity of the protein surface cannot in principle be ruled out.

In the inset of Figure 2, D versus η_{sol} is shown in a log–log scale where the power law dependence between these sets of data is evident: the fitting line corresponds to a fractional SE relation with an exponent $\alpha = 0.46 \pm 0.03$.

It would be interesting to trace back this power law behavior to the leading parameters of the concentration dependence of D and η_{sol} , i.e., k_D and $[\eta]$. This can be achieved by substituting eq 11 into eq 10 truncated to the first order in C :

$$D \approx D_0 \left[1 + k_D \left(\frac{\eta_{\text{sol}} - \eta_0}{\eta_0 [\eta]} \right) \right] \quad (13)$$

from which one can derive

$$\alpha = \lim_{C \rightarrow 0} \left| \frac{\partial \log(D)}{\partial \log(\eta_{\text{sol}})} \right|_{\eta_0} = \frac{k_D}{[\eta]} \quad (14)$$

By taking the best fit values of $[\eta]$ and k_D , one computes $\alpha = 0.48 \pm 0.08$ in very good agreement with the best fit $\alpha \approx 0.46$ found when fitting directly D vs η_{sol} . Therefore we suggest that a better understanding of the fractional SE relation, obtained when changing the protein concentration, can be gained by studying the two parameters $[\eta]$ and k_D separately.

As mentioned above, the intrinsic viscosity $[\eta]$ depends on the loss of momentum of the isolated macromolecule to the solvent since any protein–protein interaction effects has been eliminated by extrapolation to $C = 0$. $[\eta]$ depends more on the molecule structure, mass M and volume V_h , and on the intramolecular hydrodynamics, i.e., the hydrodynamic interactions between different moieties of the macromolecule, and in general,¹ is proportional to the ratio V_h/M :

$$[\eta] = \nu \frac{V_h N_{\text{av}}}{M} \quad (15)$$

where the Simha factor¹ $\nu \approx 2.5$ and M is in daltons. The hydrated radius R_h obtained by inverting eq 15 and assuming the experimental value for $[\eta]$ is 35 ± 1 Å in reasonable agreement with what found from the diffusion coefficient measurement.

The interaction constant k_D is instead affected by both the direct and hydrodynamic interactions. Though a consolidated literature exists about colloid–colloid direct interactions,¹⁹ which can be summarized by the so-called DLVO potential, the hydrodynamic interactions effects are still a matter of debate. The DLVO potential²⁰ U_{DLVO} is a composition of a screened Debye–Hückel potential, U_{DH} , a short range attractive (van der Waals) potential, U_{SR} , and an hard sphere contribution, U_{HS} . The parameters involved in describing these interactions are the protein charge Q , radius R_h , the solution ionic strength I , and the Hamaker constant H_A , related to the short-range attractive part of the potential.²¹

When considering a protein at the isoelectric point, as, in the present case, one can disregard the screened D–H potential (since $Q = 0$) and write

$$U_{\text{DLVO}}(\rho, H_A) = U_{\text{SR}}(\rho, H_A) = -\frac{H_A}{12} \left\{ \frac{1}{(1+\rho)^2} + \frac{1}{(\rho+\rho)^2} + 2 \ln \left[\frac{2\rho+\rho^2}{(1+\rho)^2} \right] \right\} \quad (16)$$

where $\rho = (r - 2R)/2R$ is the interparticle distance normalized to the particle diameter. In so doing the interparticle interactions depend on the choice of the Hamacker constant only. The direct interactions are mediated through the solvent and, depending on the type of boundary conditions, contribute to the interaction constant k_D as

$$k_D(\xi) = k_{\text{HS}}(\xi) + \int_{x_c}^{\infty} (g(\rho) - 1) F(\rho, \xi) d\rho \quad (17)$$

where $k_{\text{HS}}(\xi)$ is the hard core contribution to the interaction constant and $x_c = 0.06$ is due to the width of the hydration/Stern layer.²² The radial distribution function at the lowest order is $g(\rho, H_A) = \exp(-U_{\text{DLVO}}(\rho, H_A)/k_B T)$. The function $F(\rho, \xi)$ represents the change in the diffusional properties of the protein due to the hydrodynamic interactions, and its analytical expression depends on the type of approximation used for describing these interactions. Felderhof¹⁶ gave simple expressions for the two-body hydrodynamic interactions but did not compute the contribution due to the divergence of the hydrodynamic tensor. This term was computed, though only for stick boundary conditions, by Phillies.²³ We extend here the computation made by Phillies to the case of mixed boundary conditions finding the equations reported in the Appendix (see eq 37).

The term $k_D(\xi, H_A)$ is more relevant in the case of low protein charge and seems to be essential to describe our experimental data which corresponds to the protein isoelectric point, i.e. $Q \approx 0$. In the inset of Figure 3 we show the result of the computation (see eqs 17 and 37) of the interaction constant $k_D(\xi, H_A)$ for an uncharged BSA protein versus the Hamacker constant, H_A , for four values of the boundary condition parameter $\xi = 0, 0.1, 0.2$, and 0.3 . The value of the interaction constant does not depend much on the value of ξ , even if changes of the Hamacker constant H_A , by a factor of $k_B T$ only, implies a relevant variation of k_D .

As a matter of fact, one could predict a value very similar to the experimental one, $k_D \approx -0.019$ dL/g, either by assuming a $H_A \approx k_B T$ and $\xi = 0$, i.e., stick boundary conditions, or $H_A \approx 4 k_B T$ and $\xi = 0.3$, very close to the maximum value $\xi_{\text{max}} = 1/3$ corresponding to slip boundary conditions. This can be seen from the intercept of the curves $k_D(\xi, H_A)$ (inset of Figure 3) with the horizontal line that indicates the experimental value.

A well determined consensus value for H_A is not available. However, even if the reported values for H_A spans a wide range $0.5 k_B T \leq H_A \leq 10 k_B T$, recent works on small globular proteins^{22,24} have found relatively high values $H_A \approx 8-10 k_B T$. In the present case, the assumption of high values of H_A implies anomalous boundary conditions. However, in order to estimate a consistent value of ξ , one must fit the measured trend of the diffusion coefficient versus the protein concentration to eq 10, since also the single particle diffusion coefficient $D_0(\xi)$, and not just k_D , does depend on the boundary conditions. Values of $\mathcal{S} = 6(1 - \xi)$ may be evaluated by fitting the experimental data to eq 10 and making use of eqs 17 and 37. We assume either $H_A = 4.5 k_B T$ or $H_A = 6 k_B T$ and obtain the values of \mathcal{S} plotted in Figure 3 versus the protein concentration: a constant value $\xi \approx 0$, i.e., $\mathcal{S} = 6$ is found for $H_A \approx 2 k_B T$ (data not shown). However this latter possibility is much less probable in the view of the recent consensus value^{22,24} for $H_A \geq 5 k_B T$.

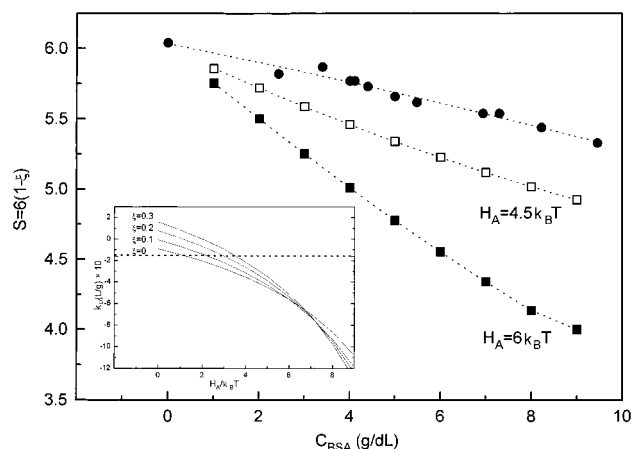


Figure 3. The values of the parameter $\mathcal{S} = 6(1 - \xi)$ obtained by fitting the experimental diffusion coefficients versus concentration to the eq 10, $D(C) = D_0(\xi) (1 + k_D(\xi)C)$, are shown for two values of the Hamacker constant H_A : $H_A = 4.5 k_B T$ (open squares) and $H_A = 6 k_B T$ (filled circles). The filled circles are the parameter \mathcal{S}_0 obtained from eq 18, $D(C) = D_0(\xi)$, in the text. Inset: computed values of k_D versus the Hamacker constant H_A at four different values of the boundary condition parameter $\xi = 0, 0.1, 0.2$, and 0.3 . The horizontal line indicate the experimental value for k_D .

Neglecting the interaction effect, i.e., k_D in eq 10, leads to underestimating the degree of slip boundary conditions as demonstrated by the comparison of \mathcal{S} to the values that can be obtained by inverting the following phenomenological relation:

$$D = \frac{k_B T}{\pi \eta_{\text{sol}} R \mathcal{S}_0} \quad (18)$$

The comparison of this equation to eq 7 shows that \mathcal{S}_0 is overestimated with respect to \mathcal{S} due to a term $\approx 1 + (k_D + [\eta]C)$, which, for the maximum concentration $C \approx 10$ g/dL, corresponds to ≈ 1.2 as found in Figure 3.

V. Conclusions

The protein diffusion coefficient and the solution viscosity have been simultaneously monitored by PCS as a function of the protein concentration. By this method, which allows low shear rate viscosity measurements, we have put into evidence a fractional Stokes–Einstein relation $D \sim 1/\eta_{\text{sol}}^\alpha$. The power law exponent α has been traced back to the interparticle interactions and the protein size through an analysis of the parameters k_D and $[\eta]$.

When taking into account interactions effects on k_D , the observed trend of the diffusion coefficient versus the protein concentration is consistent with protein–solvent boundary conditions which are changing gradually from the stick to the slip case as the potential–protein distance decreases.

Though it is not easy to estimate the exact amount of the degree of slip boundaries due to the still relatively high uncertainty in H_A , the picture we propose suggests protein-induced perturbations of the solvent structure, which may overlap at increasing protein volume fraction.

VI. Appendix

The aim of this appendix is to show how to compute the contribution due to the divergence of the hydrodynamic tensor to the mutual diffusion in the case of mixed stick–slip boundary conditions. This is necessary in order to correctly evaluate the hard sphere contribution to the diffusion interaction constant,

i.e., k_{HS} , for general boundary conditions. The result of this appendix (see eq 37), is then used in eqs 10 and 17 when fitting the experimental diffusion data (see Figure 2). The appendix follows the guidelines of the papers by Phillies²⁵ and Felderhof.¹⁶

The computation of the mutual diffusion coefficient of a protein of radius a , to the first order in the number concentration n , and for a generic boundary condition (i.e., $0 \leq \xi \leq 1/3$), follows the equation²⁵

$$D(\xi) = D_0(1 - \xi)[1 + n(A_D + B_D)] \quad (19)$$

where

$$A_D = \int d^3\mathbf{r} g(r) \hat{\mathbf{k}} \cdot \nabla \xi \cdot \hat{\mathbf{k}} \quad (20)$$

and

$$B_D = \frac{\hat{\mathbf{k}}}{k} \int d^3\mathbf{r} g(r) e^{i\mathbf{k} \cdot \mathbf{r}} \nabla : \nabla \xi \quad (21)$$

where $g(r)$ is the protein–protein radial distribution function, \mathbf{k} indicates the scattering vector, and $\nabla \xi$ is the hydrodynamic tensor as given by Felderhof.¹⁶

$$\nabla \xi = \mathcal{A}(\xi) + \mathcal{B}(\xi) \quad (22)$$

where

$$\mathcal{A}(\xi) = D_0(1 - \xi) \left[-\frac{15}{4} \left(\frac{1 - \xi}{1 + 2\xi} \right) \left(\frac{a}{r} \right)^4 \hat{\mathbf{r}} \cdot \hat{\mathbf{r}} + \frac{1}{16} \left(\frac{a}{r} \right)^6 (\hat{\mathbf{r}} \cdot \hat{\mathbf{r}} f_p(\xi) - f_l(\xi) \mathbf{I}) \right] \quad (23)$$

where

$$f_p(\xi) = 192 \left(\frac{1 - 3\xi}{1 + 2\xi} \right) - \frac{483}{5} \left(\frac{1 - \xi}{1 + 4\xi} \right) + 12 \left(\frac{1 - 4\xi}{1 + \xi} \right) - 12 \left(\frac{1 - 6\xi}{1 - \xi} \right) \quad (24)$$

and

$$f_l(\xi) = -\frac{21}{5} \left(\frac{1 - \xi}{1 + 4\xi} \right) - 12 \left(\frac{1 - 4\xi}{1 + \xi} \right) + \frac{4}{5} \left(\frac{1 - 6\xi}{1 - \xi} \right) \quad (25)$$

The second term in eq 22 is given by

$$\mathcal{B}(\xi) = D_0(1 - \xi) \left[-\frac{3}{4} \left(\frac{a}{r} \right) (\mathbf{I} + \hat{\mathbf{r}} \cdot \hat{\mathbf{r}}) + \frac{1}{2} \left(\frac{a}{r} \right)^3 \left(\frac{1 - 3\xi}{1 - \xi} \right) (\mathbf{I} - 3\hat{\mathbf{r}} \cdot \hat{\mathbf{r}}) + \frac{75}{4} \left(\frac{a}{r} \right)^7 \left(\frac{1 - \xi}{1 + 2\xi} \right)^2 \hat{\mathbf{r}} \cdot \hat{\mathbf{r}} \right] \quad (26)$$

The first term in eq 19 has been already computed by Felderhof¹⁶ for an undefined boundary condition, while the second term, proposed by Phillies,²⁵ has been computed for the stick boundary condition only. The purpose of this appendix is to show the correction term due to a generic boundary condition to the divergence term in eq 19.

By applying the definition of the divergence of a tensor $T_{\alpha\beta}$, i.e., $(\nabla : T)_{\alpha} = \partial/\partial r_{\beta} T_{\beta\alpha}$, to eq 22 one can show that

$$\nabla : \nabla \xi = \mathbf{r} F(\mathbf{r}, \xi) \quad (27)$$

with

$$a^2 F(\mathbf{r}, \xi) = D_0(1 - \xi) \left[\left(\frac{a}{r} \right)^6 f_6(\xi) + \left(\frac{a}{r} \right)^8 f_8(\xi) + \left(\frac{a}{r} \right)^9 f_9(\xi) + \dots \right] \quad (28)$$

and

$$f_6(\xi) = \frac{15}{2} \left(\frac{1 - \xi}{1 + 2\xi} \right) \quad (29)$$

$$f_8(\xi) = -48 \left(\frac{1 - 3\xi}{1 + 2\xi} \right) + \frac{1029}{40} \left(\frac{1 - \xi}{1 + 4\xi} \right) + \frac{9}{10} \left(\frac{1 - 6\xi}{1 - \xi} \right) + \frac{3}{2} \left(\frac{1 - 4\xi}{1 + \xi} \right) \quad (30)$$

$$f_9(\xi) = -\frac{375}{4} \left(\frac{1 - \xi}{1 + 2\xi} \right)^2 \quad (31)$$

The computation of the second integral of eq 19 is based on the special form of the divergence of the hydrodynamic tensor. One can write

$$in_0 \frac{\hat{\mathbf{k}}}{k} \int d^3\mathbf{r} g(r) \nabla : \nabla \xi e^{i\mathbf{k} \cdot \mathbf{r}} = \frac{n_0}{k^2} \int_0^{\infty} dr r^2 2\pi g(r) ikr \times \int_{-1}^{+1} d\mu F(\xi, r) \mu e^{ikr\mu} = -\frac{n_0 4\pi}{k} \int_0^{\infty} dr r^3 g(r) F(\xi, r) j_1(kr) \quad (32)$$

A further simplification of the previous expressions can be obtained when considering that the integrand has nonvanishing values for interparticle distances of some protein radius (typically $\approx 2 - 20$ nm), and the scattering vector is the order of 10^{-2} nm^{-1} with visible radiation. This means that the argument of the spherical Bessel function $j_1(x)$ can be approximated to $x \approx 0$, obtaining $j_1(x) \approx x/3$. Equation 32 becomes

$$in_0 \frac{\hat{\mathbf{k}}}{k} \int d^3\mathbf{r} g(r) \nabla : \nabla \xi e^{i\mathbf{k} \cdot \mathbf{r}} \approx -vn_0 \int_0^{\infty} d\left(\frac{r}{a}\right) \left(\frac{r}{a}\right)^4 g(r) a^2 F(\xi, r) \quad (33)$$

where v is the molecular volume.

One must go further in evaluating the contribution of the hard sphere part of the interaction energy and split the above integral in two terms of the type:

$$\begin{aligned} \int_0^{\infty} dr g(r) H(r) &= \int_0^{2a} dr (g(r) - 1) H(r) + \int_{2a}^{\infty} dr (g(r) - 1) H(r) + \int_0^{2a} dr H(r) \\ &= -\int_0^{2a} dr H(r) + \int_{2a}^{\infty} dr (g(r) - 1) H(r) + \int_0^{\infty} dr H(r) \\ &= \int_{2a}^{\infty} dr H(r) + \int_{2a}^{\infty} dr (g(r) - 1) H(r) \\ &= 2a \int_0^{\infty} d\rho H(2a(1 + \rho)) + 2a \times \\ &\quad \int_0^{\infty} d\rho (g(2a(1 + \rho)) - 1) H(2a(1 + \rho)) \quad (34) \end{aligned}$$

where $H(r)$ indicates a generic function to be weighted over the radial distribution function and ρ is a normalized particle–particle distance $\rho = (r - 2a)/2a$. The first integral of the last equation corresponds to the hard sphere contribution. Finally, by applying eq 34 to eq 33, a simplified form of the divergence term in eq 19 can be obtained

$$in_0 \frac{\hat{\mathbf{k}}}{k} \cdot \int d^3\mathbf{r} g(r) \nabla : \nabla \xi e^{i\mathbf{k} \cdot \mathbf{r}} = -n_0 v (\lambda_{\text{div}} + \lambda_{\text{div,HS}}) = C(k_{\text{div}} + k_{\text{div,HS}}) \quad (35)$$

where

$$k_{\text{div}} = -\bar{v} \int_0^{\infty} d\rho (1 + \rho)^4 (g(\rho) - 1) F_D(\xi, \rho)$$

and

$$F_D(\xi, \rho) = (1 - \xi) \left[(1 - \rho)^{-6} \frac{f_6(\xi)}{2} + (1 - \rho)^{-8} \frac{f_8(\xi)}{8} + (1 - \rho)^{-9} \frac{f_9(\xi)}{16} \right]$$

We have indicated the partial molecular volume as \bar{v} . Finally the hard sphere contribution for the divergence term is given by

$$k_{\text{div,HS}} = -\bar{v}(1 - \xi) \left[\frac{f_6(\xi)}{2} + \frac{f_8(\xi)}{24} - \frac{f_9(\xi)}{64} \right] \quad (36)$$

In order to compute the full dependence of the mutual diffusion coefficient upon the protein concentration in the general boundary conditions case, one computes the first integral in eq 19 following the guide lines given by Felderhof¹⁶ and Phillies.²³ The only difference between the two treatments is the presence of a term of the type $-(1 - \xi)$ in the hard sphere part of the λ coefficient due to the sum rule. In particular, the total hard sphere concentration dependence of D is given by

$$k_{\text{HS}} = \bar{v}8 + \bar{v}(1 - \xi) \left[1.5g_4(\xi) + 0.125g_6(\xi) + \frac{75}{256} \left(\frac{1 - \xi}{1 + 2\xi} \right)^2 - 6 + \frac{1 - 3\xi}{1 - \xi} - 1 - \frac{f_6(\xi)}{2} - \frac{f_8(\xi)}{24} - \frac{f_9(\xi)}{64} \right] \quad (37)$$

where

$$g_4(\xi) = -\frac{5}{4} \frac{1 - \xi}{1 + 2\xi} \quad (38)$$

and

$$g_4(\xi) = 4 \left(\frac{1 - 3\xi}{1 + 2\xi} \right) - \frac{91}{40} \left(\frac{1 - \xi}{1 + 4\xi} \right) - \frac{1}{10} \left(\frac{1 - 6\xi}{1 - \xi} \right) - \frac{1}{2} \left(\frac{1 - 4\xi}{1 + \xi} \right) \quad (39)$$

References and Notes

- (1) Cantor, C.; Schimmel, P. *Biophysical Chemistry*; Academic Press: New York, 1980.
- (2) Fischer, E. W. *Phys. A* **1993**, *201*, 183.
- (3) Hodgdon, J. A.; Stillinger, F. H. *Phys. Rev. E* **1993**, *48*, 207.
- (4) Angell, C. *Science* **1995**, *267*, 1924.
- (5) Bartsch, E.; Frenz, V.; Sillescu, H. *J. Non-Cryst. Solids* **1994**, *172*, 88.
- (6) Stellbrink, J.; Allgaier, J.; Richter, D. *Phys. Rev. E* **1997**, *56*, 3772.
- (7) Placidi, M.; Cannistraro, S. *Europhys. Lett.* **1988**, *43*, 476.
- (8) Gregory, R. B. *Protein-Solvent Interactions*; Marcel Dekker: New York, 1995.
- (9) Fine, B. M.; Pande, J.; Lomakin, A.; Ogun, O. O.; Benedek, J. B. *Phys. Rev. Lett.* **1995**, *74*, 198.
- (10) Voronel, A.; Veliyulin, E.; Machavariani V. Sh. *Phys. Rev. Lett.* **1988**, *80*, 2630.
- (11) Lamanna, R.; Delmelle, M.; Cannistraro, S. *Phys. Rev. E* **1994**, *49*, 5878.
- (12) Dixon, P.; Nagel, S. *J. Chem. Phys.* **1991**, *94*, 6924.
- (13) Almog, Y.; Brenner, H. *Phys. Fluids* **1997**, *9*, 16.
- (14) Koppel, D. E. *J. Chem. Phys.* **1972**, *57*, 4814.
- (15) Wilcoxon, J. *Biopolymers* **1983**, *22*, 1023.
- (16) Felderhof, B. U. *Phys. A* **1997**, *89*, 373.
- (17) Batchelor, G. K. *J. Fluid Mech* **1977**, *74*, 1.
- (18) Doi, M.; Edwards, S. F. *Theory of Polymer Dynamics*; Clarendon Press: Oxford, 1988.
- (19) Neal, D. G.; Purich, D.; Cannel, D. S. *J. Chem. Phys.* **1984**, *80*, 3469.
- (20) Dhont, J. K. G. *An Introduction to Dynamics of Colloids*; Elsevier: Amsterdam, 1996.
- (21) Corti, M.; Degiorgio, V. *J. Phys. Chem.* **1981**, *85*, 711.
- (22) Kuehner, D. E.; Heyer, C.; R  msch, C.; Fornefeld, U. M.; Blanch, H. W.; Prausnitz, J. M. *Biophys. J.* **1997**, *73*, 3211.
- (23) Phillies, G. D. J. *J. Phys. Chem.* **1995**, *99*, 4265.
- (24) Muschol, M.; Rosenberger, F. *J. Chem. Phys.* **1995**, *103*, 10424.
- (25) Phillies, G. D. J. *J. Colloid Interface Sci.* **1987**, *119*, 518.